International Journal of Physics and Applications

E-ISSN: 2664-7583
P-ISSN: 2664-7575
IJOS 2023; 5(1): 13-18

www.physicsjournal.in
Received: 06-11-2022
Accepted: 19-12-2022

Ch Atchyutha Rao
Department of Physics, GDC-Nakkapalli, Anakapalle (Dt) Andhra Pradesh, India

N Bujji Babu
Department of Chemistry, PR Government Degree College (A), Kakinada, Andhra Pradesh, India

KVR Murthy
Display Materials Laboratory, Department of Applied Physics, Faculty of Technology and Engineering, M. S. University of Baroda, Vadodara, Gujarat, India

Corresponding Author:
Ch Atchyutha Rao
Department of Physics, GDC-Nakkapalli, Anakapalle (Dt) Andhra Pradesh, India

Photoluminescence study of rare earth ions doped Sr_2CeO_4 phosphor prepared via conventional solid-state reaction method

CH Atchyutha Rao, N Bujji Babu and KVR Murthy

DOI: https://doi.org/10.33545/26647575.2023.v5.i1a.57

Abstract
The lanthanide ions either in their divalent or trivalent charge state form a very important class of luminescence activators in phosphors and single crystals. Doping these lanthanide ions in different host lattices are widely utilized in many areas for example the 5d-4f emission of Ce^{3+} used in scintillators for γ-ray detection, cathode ray tubes and electroluminescence phosphors. The photon cascade emission from $4f^2$ levels of Pr^{3+} used for developing high quantum efficiency phosphors excited by means of a Xe discharge in the vacuum-UV. The narrow line $4f^3$ transition in Nd^{3+} is used in laser crystals. The Sm^{3+} emission used as an electron trap and in information storage properties like optical memory applications, X-ray imaging phosphor applications. The famous $^5D_0$-^7F_j $4f^6$ redline emission of Eu^{3+} and the blue to red 5d-4f emission of Eu^{2+} are used in display and lighting phosphors. The $4f^8$ line emission of Tb^{3+} is used in tricolor tube lighting. The Dy^{3+} emission plays an important role in the persistent luminescence phosphors. Er^{3+}, Tm^{3+} used to investigate for possible photon cascade emission phosphor applications. This is brief and still incomplete summary illustrates the diversity of applications involving the luminescence of lanthanide ions.

Keywords: Strontium cerium oxide (Sr_2CeO_4) phosphor, rare earth ion, conventional solid-state reaction method

1. Introduction
The trivalent ions of the lanthanide series are characterized by a gradual filling of the 4f orbital, from $4f^0$ (for La^{3+}) to $4f^{14}$ (for Lu^{3+}) and shown in table 1. One of the most interesting features of these ions is their photoluminescence. Several lanthanide ions show luminescence in the visible or near-infrared spectral regions upon irradiation with ultraviolet radiation. The color of the emitted light depends on the lanthanide ion. For instance, Eu^{3+} emits red light, Tb^{3+} green light, Sm^{3+} orange light, and Tm^{3+} blue light. Yb^{3+}, Nd^{3+}, and Er^{3+} are well-known for their near-infrared luminescence, but other lanthanide ions (Pr^{3+}, Sm^{3+}, Dy^{3+}, Ho^{3+}, and Tm^{3+}) also show transitions in the near-infrared region. Gd^{3+} emits in the ultraviolet region, but its luminescence can only be observed in the absence of organic ligands with low-lying singlet and triplet levels [1-3]. When the light emission by lanthanide ions is discussed, one often uses the term 'luminescence', rather than the terms 'fluorescence' or 'phosphorescence'. The emission mechanism: *fluorescence* is singlet-to-singlet emission (i.e., a spin-allowed transition) and *phosphorescence* is triplet-to-singlet emission (i.e., a spin forbidden transition). The lanthanide rare earths' electronic configuration consists of a filled xenon core and 6*s* shells, followed by filling of 5*d* and 4*f* shells. The interesting feature of the lanthanide series is that their 4*f* shell begins to fill after 6*s*. In addition, the 4*f* shell, instead of having a radius larger than the 5*s* and 5*p* shells, actually contracts and becomes bounded by these shells. The trivalent state is formed by removal of two of the 6*s* electrons and one of the 4*f* electrons, with the outer 5*s* and 5*p* shells remaining intact [4-7]. This configuration renders the 4*f* electronic levels less sensitive to the glass or crystal host site environment. The optical spectrum of the trivalent ions of lanthanide rare earths consists of various excited states of the 4*f* electrons. The spread in the $4f^N$ transitions spectra arises from various atomic interactions between the electrons, and Stark splitting due to the host environment [8-12]. In the case of the lanthanides, the emission is due to transitions inside the 4f shell, thus intra-configurationally f-f transitions. Because the partially filled 4f shell is well shielded from its environment by the

closed $5s^2$ and $5p^6$ shells, the ligands in the first and second co-ordination sphere perturb the electronic configurations of the trivalent lanthanide ions only to a very limited extent. This shielding is responsible for the specific properties of lanthanide luminescence, more particularly for the narrowband emission and for the long lifetimes of the excited states. Ce^{3+} is a special case because this ion emits intense broadband emission due to allowed f-d transitions. The position of the emission maximum strongly depends on the ligands environment of the Ce^{3+} ion [9-15, 26].

Table 1: Electronic structure of the trivalent lanthanide ions

Element	Symbol	Atomic number (Z)	Configuration Ln^{3+}	Ground state Ln^{3+}
Lanthanum	La	57	$[Xe]4f^0$	$^1S_0$
Cerium	Ce	58	$[Xe]4f^2$	$^2F_{5/2}$
Praseodymium	Pr	59	$[Xe]4f^3$	$^3H_4$
Neodymium	Nd	60	$[Xe]4f^4$	$^4I_{9/2}$
Promethium	Pm	61	$[Xe]4f^5$	$^5I_4$
Samarium	Sm	62	$[Xe]4f^6$	$^6H_{5/2}$
Europium	Eu	63	$[Xe]4f^7$	$^7F_0$
Gadolinium	Gd	64	$[Xe]4f^8$	$^8S_{7/2}$
Terbium	Tb	65	$[Xe]4f^9$	$^7F_6$
Dysprosium	Dy	66	$[Xe]4f^{10}$	$^6H_{15/2}$
Holmium	Ho	67	$[Xe]4f^{11}$	$^5I_8$
Erbium	Er	68	$[Xe]4f^{12}$	$^4I_{15/2}$
Thulium	Tm	69	$[Xe]4f^{13}$	$^3H_6$
Ytterbium	Yb	70	$[Xe]4f^{14}$	$^2F_{7/2}$
Lutetium	Lu	71	$[Xe]4f^{14}$	$^1S_0$

2. Experimental work

The present paper reports on the synthesis and characterization of rare earth ions doped Sr_2CeO_4 phosphor, using solid state reaction method. The compounds like Strontium Carbonate ($SrCO_3$), Cerium Oxide (CeO_2) and (La^{3+}, Pr^{3+}, Nd^{3+}, Sm^{3+}, Eu^{3+}, Gd^{3+}, Tb^{3+}, Dy^{3+} and Er^{3+}) (Sigma-Aldrich Chemie Inc., Germany) in the oxide form of high purity of analytical grade exceeding (99.9% assay) chemicals were used as starting materials. First we prepared Sr_2CeO_4 phosphor, without adding any dopants, as host material by weighing, adding Strontium carbonate ($SrCO_3$) (Sigma-Aldrich Chemie Inc., Germany), Cerium Oxide (CeO_2) (National Chemicals, Vadodara, India) were used as starting materials for the host material taken in stoichiometric proportions of Sr: Ce as 2:1 and ground into a fine powder using agate mortar and pestle about an hour. The grounded sample was placed in an alumina crucible and fired at 1200°C for 3 hours in a muffle furnace with a heating rate of 5°C/min. The sample is allowed cool to room temperature in the same furnace for about 20 hours. In the same way rare earth (RE) ions (La^{3+}, Pr^{3+}, Nd^{3+}, Sm^{3+}, Eu^{3+}, Gd^{3+}, Tb^{3+}, Dy^{3+} and Er^{3+}) are doped at 0.5mol% concentration only.

We investigated the phase purity, morphology, Photoluminescence excitation and emission and CIE color co-ordinates. XRD analysis was carried out with a powder diffractometer (Rigaku-D/max 2500) using Cu Kα radiation, microstructures/morphology of the samples were studied using a scanning electron microscopy (Philips XL-CP-30), Photoluminescence emission and excitation spectra were measured by Spectro fluorophotometer (SHIMADZU, RF-5301 PC) using Xenon lamp as excitation source, All the spectra were recorded at room temperature. Emission and excitation spectra were recorded using a spectral slit width of 1.5nm. The Commission International de l'Eclairage (CIE-1931 chromaticity diagram) color co-ordinates were calculated by the spectrophotometric method using the spectral energy distribution. The chromatic color coordinates (x, y) of prepared materials was calculated with colour calculator version 2, software from Radiant Imaging [17].

3. Results and Discussion

3.1 XRD Analysis

X-ray powder diffraction (XRD) of un-doped Sr_2CeO_4 phosphor was carried out at room temperature. Fig.1 shows XRD Pattern of un-doped Sr_2CeO_4 phosphor. From the XRD pattern analysis it was found that the prominent phase formed is Sr_2CeO_4 phosphor, after the computer program POWD (an interactive Powder diffraction Data Interpretation and Indexing Program, Version 2.2) was used to calculated hkl and d values were found to be in good agreement with the JCPDS data card No. 50-0115. This reveals that the structure of Sr_2CeO_4 is orthorhombic and is in agreement with the findings of the previous workers like Sankar *et al.* [18], Danielson *et al*. However the data reported by Jiang *et al.* [20] and Serra *et al.* [21] indicate triclinic structure. It clearly indicates that the heat treatment temperature and time of cooling were sufficient to form single phase. The calculated lattice parameters are a = 6.094 Å, b = 10.232 Å, c = 3.566 Å, and volume V = a*b*c = 6.094*10.232*3.566 = 222.354 $Å^3$. The crystallite size was determined using the Scherrer's equation $D = k\lambda / \beta \cos\theta$, where k the constant (0.94), λ the wavelength of the X-ray (0.154 nm or 1.54 Å), β the full-width at half maxima (FWHM) and θ the Bragg angle of the XRD peak (1,1,1). The calculated average crystallite size of un-doped Sr_2CeO_4 is ~ 28 nm.

Fig.2 shows XRD pattern of rare earth (RE^{3+}) ions (La^{3+}, Pr^{3+}, Nd^{3+}, Sm^{3+}, Eu^{3+}, Gd^{3+}, Tb^{3+}, Dy^{3+} and Er^{3+}) doped Sr_2CeO_4 phosphor at 0.5mol% concentration. All the diffraction peaks are looking same as un-doped Sr_2CeO_4 phosphor, concluding that the dopant ions did not affect the host structure except the increase or decrease of intensity. The calculated average crystallite sizes of Sr_2CeO_4 doped RE^{3+} phosphors are shown in the table. 2.

Table 2: The calculated average crystallite sizes of Sr_2CeO_4 doped RE^{3+} phosphors

S. No.	Rare earth ion	Average Crystallite size (nm)
1	Un-doped Sr_2CeO_4	28
2	Sr_2CeO_4: La^{3+}	23
3	Sr_2CeO_4: Pr^{3+}	25
4	Sr_2CeO_4: Nd^{3+}	29
5	Sr_2CeO_4: Sm^{3+}	30
6	Sr_2CeO_4: Eu^{3+}	31
7	Sr_2CeO_4: Gd^{3+}	23
8	Sr_2CeO_4: Tb^{3+}	26
9	Sr_2CeO_4: Dy^{3+}	29
10	Sr_2CeO_4: Er^{3+}	22

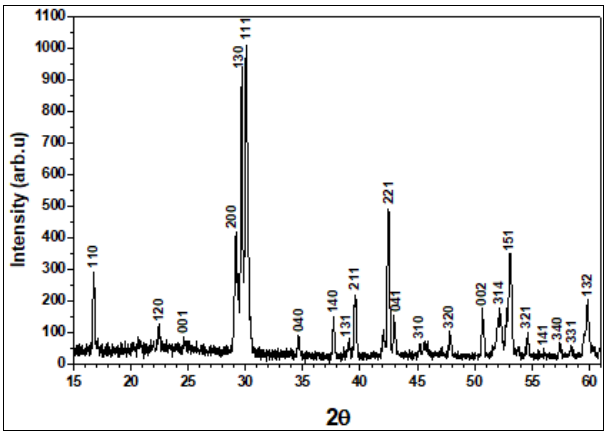

Fig 1: XRD Pattern of un-doped Sr_2CeO_4 phosphor

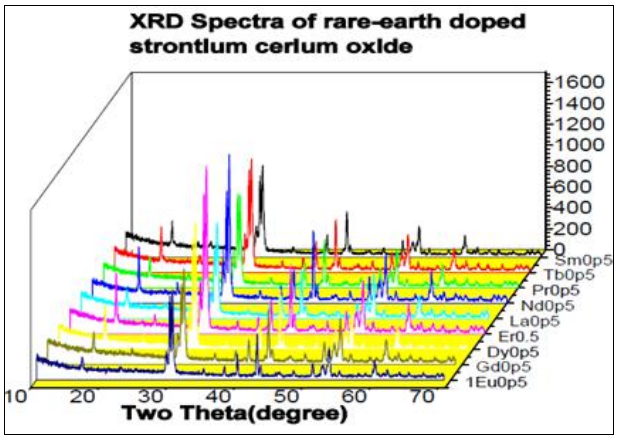

Fig 2: XRD Pattern of RE^{3+} ions doped Sr_2CeO_4 phosphor

3.2 Photoluminescence Study

The excitation and emission spectra recorded for un-doped Sr_2CeO_4 at room temperature are presented in Fig.3. The excitation spectrum monitored at ~400 nm shows a broad band with one maximum at 280 nm. The feature of the excitation spectrum changed when monitored at ~ 470 nm shows a broad band with two maxima at 280 and 350 nm. These bands have been assigned as intra configurationally Ce^{4+}– O^{2-} charge transfer (CT) transitions by Danielson *et al.* [22]. The emission spectra recorded on exciting at 254, 260, 280 as well as 350 nm show a broad band with the maximum in the blue–green region (FWHM~86) with extended emission into longer wavelengths. It is well known that the CT transition is sensitive to ligand environment i.e. the potential field of the ligands. In order to find out how the next-nearest-neighbor (NNN) of the central metal ion Ce^{4+}, affects the Ce^{4+}– O^{2-} CT transition, Sr_2CeO_4 phosphor has been doped with other rare-earth (RE) ions e.g. La^{3+}, Pr^{3+}, Nd^{3+}, Sm^{3+}, Eu^{3+}, Gd^{3+}, Tb^{3+}, Dy^{3+} and Er^{3+}. These ions have unique CT associated excited states in their complexes with halogen ligands or in oxides.

$Sr_2Eu_xCeO_4$ with low concentrations of Eu^{3+} (x=1.5mol %) showed white emission whereas red luminescence occurred at higher concentrations (x= >3). The excitation spectra recorded by fixing the highest intensity Eu^{3+} emission as the monitoring wavelength show the same features for all the compositions. Fig.4 presents the excitation and emission spectra for the composition (RE x=0.5mol %). The spectra show a broad band peaking at 280 nm and a broad and sharp shoulder at 350 nm, which are already assigned to the Ce^{4+}–O^{2-} CT transition in un-doped Sr_2CeO_4 phosphor [23]. In addition, the sample shows the characteristic intra configuration 4f – 4f transitions of the Eu^{3+} ion. $^7F_0 \rightarrow {}^5L_6$ transition at 395nm and $^7F_0 \rightarrow {}^5D_2$ transition at 467nm, of these two lines 467nm is the strongest and well matched with the blue LED chip.

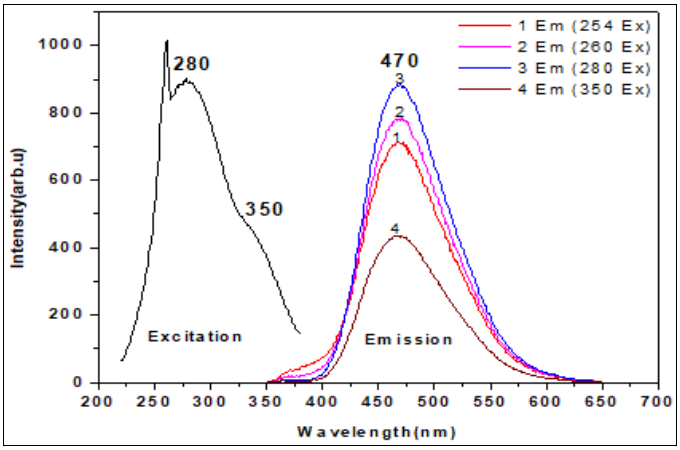

Fig 3: XRD Pattern of un-doped Sr_2CeO_4 phosphor

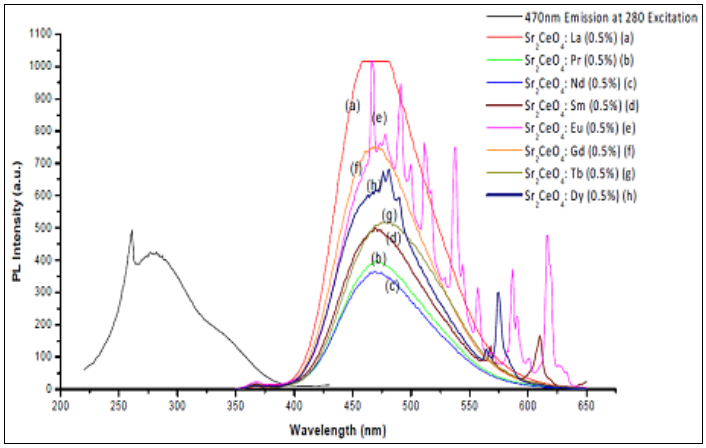

Fig 4: Excitation & Emission spectrum of RE^{3+} ions doped Sr_2CeO_4 phosphor

The emission spectrum of RE^{3+} ion doped Sr_2CeO_4 phosphor is composed of a broad band of lower intensity in the green-blue spectral region (which is already observed in the un-doped Sr_2CeO_4 phosphor) that overlaps with a set of Eu^{3+} intra-$^4f_6$ sharp lines in the blue, green and red regions. They are assigned to the transitions between the $^5D_0$, $^5D_1$ and $^5D_2$ excited states and $^7F_{0-3}$ ground level multiplets (Table. 2). The observed intra-$^4f_6$ transitions are mainly of electric-dipole (ED) nature except the $^5D_0 \rightarrow {}^7F_1$, $^5D_1 \rightarrow {}^7F_0$ and $^5D_2 \rightarrow {}^7F_1$lines, which have predominant magnetic-dipole (MD) contribution. The low intensity of $^5D_0 \rightarrow {}^7F_0$ line is because of the fact that this transition is forbidden by both ED as well as MD selection rules. According to the MD transition is relatively independent of the kind of ligands as well as the symmetry of the coordination polyhedron around the lanthanide ions [24]. The intensities of the induced ED transitions in lanthanide ions are not much affected by the environment. However the transitions, which are very sensitive to the environment, are known as hypersensitive transitions. For Eu^{3+}, $^5D_2 \rightarrow {}^7F_0$, $^5D_1 \rightarrow {}^7F_1$ and $^5D_0 \rightarrow {}^7F_2$ transitions are indicated as hypersensitive by the relative intensities of the MD transitions remain the same for all the compositions. However, drastic changes are noticed in the relative intensities of the hypersensitive transitions.

Table 3: Transitions of RE^{3+} ions doped in Sr_2CeO_4 Phosphor

S. No	Dopant	λ (nm)	I_{emi}	Transitions
1.	La	467	1005	$^4F_{9/2} \rightarrow {}^4I_{15/2}$
2.	Pr	467	755	$^3P_0 \rightarrow {}^3H_4$
3.	Nd	467	635	$^4F_{9/2} \rightarrow {}^4I_{9/2}$
4.	Gd	469	535	$^6P_{7/2} \rightarrow {}^8S_{7/2}$
5.	Tb	475	395	$^5D_4 \rightarrow {}^7F_6$
6.	Sm	565	165	$^4G_{5/2} \rightarrow {}^6H_{5/2}$
		610	222	$^4G_{5/2} \rightarrow {}^6H_{7/2}$
7.	Dy	480	936	$^4F_{9/2} \rightarrow {}^6H_{15/2}$
		564	191	$^4F_{9/2} \rightarrow {}^6H_{13/2}$
		573	526	$^4F_{9/2} \rightarrow {}^6H_{11//2}$
8.	Eu	467	1020	$^5D_2 \rightarrow {}^7F_0$
		491	1020	$^5D_2 \rightarrow {}^7F_2$
		513	892	$^5D_2 \rightarrow {}^7F_3$
		538	923	$^5D_1 \rightarrow {}^7F_1$
		556	372	$^5D_1 \rightarrow {}^7F_2$
		587	465	$^5D_0 \rightarrow {}^7F_1$
		617	540	$^5D_0 \rightarrow {}^7F_2$

3.3 Scanning Electron Microscopy study

Fig.5 presents the scanning electron microscopy (SEM) images of un-doped and RE^{3+} (0.5mol %) ions doped Sr_2CeO_4 Phosphor. The entire sample exhibits grain like morphology with different sizes and shape. At low and high enough magnification the particles appear agglomerated; the nature of individual crystallites is evident. Particle size is estimated through this analysis as uniformity of the particle shape and size affects the luminescence efficiency of phosphor materials [25]. From the SEM images of un-doped and RE^{3+} (0.5mol %) ions doped Sr_2CeO_4 Phosphor reveal that particles are highly agglomerated and non-uniform size estimated particles are appeared. However all the Bessel diameters are around in 10-2µm range; which can be helpful for display device technological applications in LEDs.

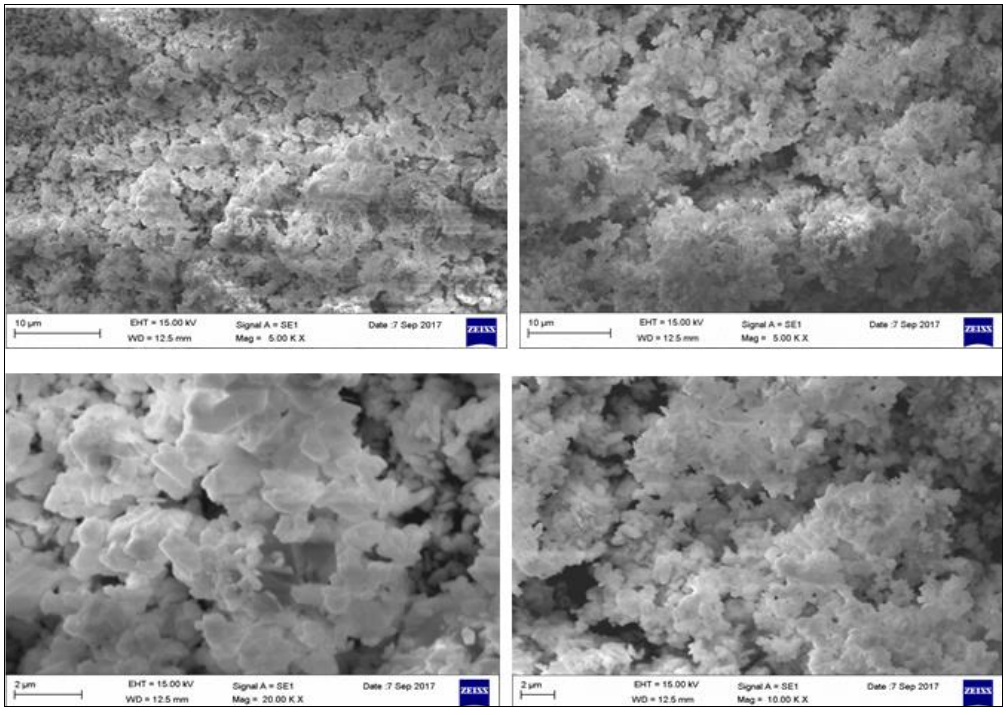

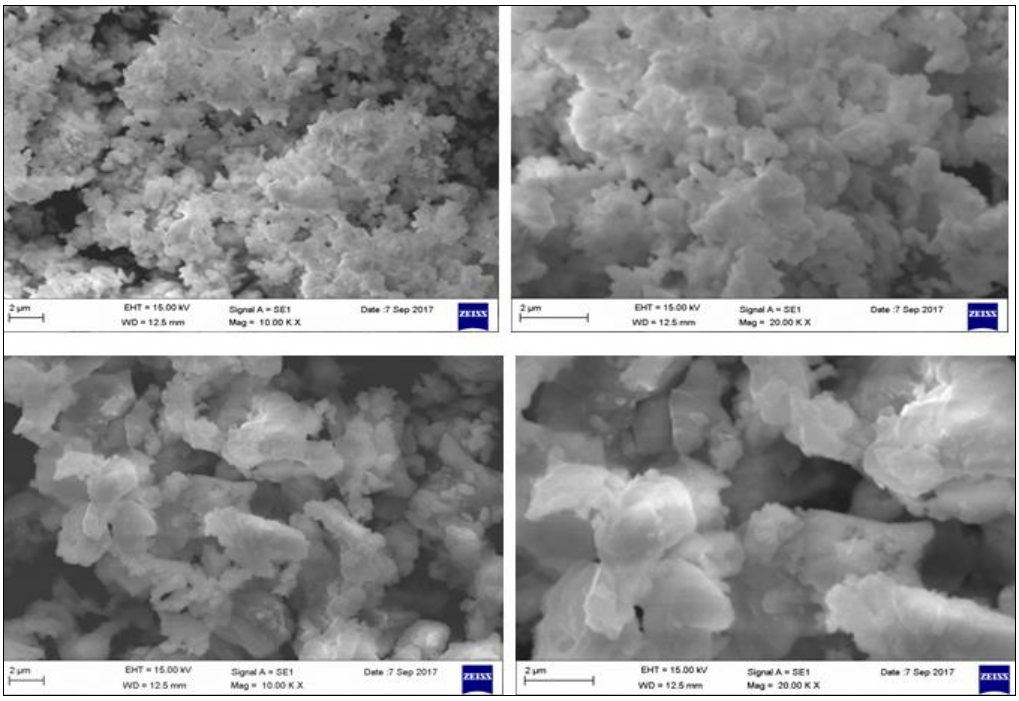

Fig 5: SEM images of un-doped & RE^{3+} (0.5mol %) ions doped Sr_2CeO_4 Phosphor

3.4 CIE Coordinates (1931 Chart)

Fig.6 Shows the CIE Colour coordinates of (1931chart) the un-doped and RE^{3+} (0.5mol %) ions doped Sr_2CeO_4 Phosphor. The present CIE Colour coordinates of (1931chart) the un-doped and RE^{3+} (0.5mol %) ions doped Sr_2CeO_4 Phosphor emitting with different colours like as blue, green, yellow and red regions under the excitation of 280, 350 nm respectively.

The CIE chromaticity coordinates for the un-doped and RE^{3+} (0.5mol %) ions doped Sr_2CeO_4 Phosphor excited at different wavelengths are summarized in table.3. The un-doped and RE^{3+} (0.5mol %) ions doped Sr_2CeO_4 Phosphors can be utilized for many applications. These single host lattices emitting white light under UV and nUV excitations is an interesting phenomenon. Hence, these phosphors are multifunctional phosphors, which one can use according to the need.

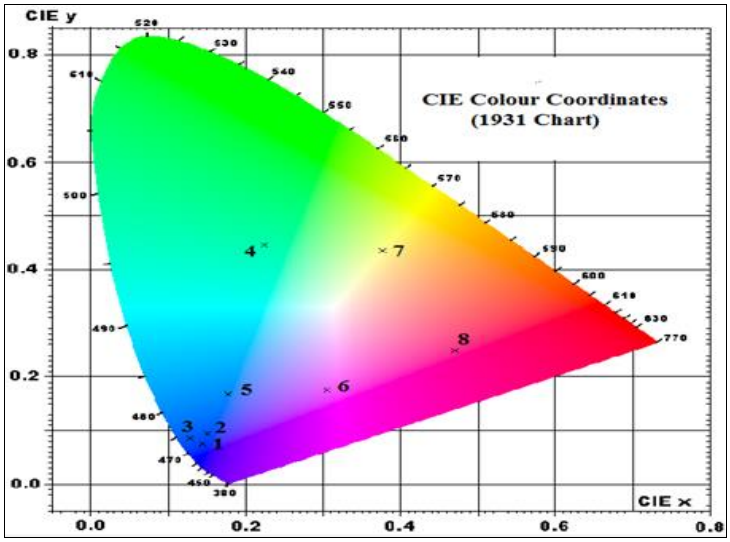

Fig 6: CIE Chromaticity diagram of un-doped & RE^{3+} (0.5mol %) ions doped Sr_2CeO_4 Phosphor

Table 4: Show the coordinates and colour region

S. No	Dopant	Coordinates		Colour Region
		X	Y	
1.	La	0.151	0.092	Blue
2.	Pr	0.145	0.075	Blue
3.	Nd	0.128	0.086	Deep Blue
4	Gd	0.224	0.445	Green
5.	Tb	0.178	0.168	Blue
6.	Sm	0.305	0.177	Bluish Red
7.	Dy	0.377	0.435	Yellow
8.	Eu	0.470	0.250	Red

4. Conclusions

- From the XRD pattern analysis it was found that the prominent phase formed is Sr_2CeO_4 phosphor, after the computer program POWD were found to be in good agreement with the JCPDS data card No. 50-0115.
- This reveals that the structure of Sr_2CeO_4 is orthorhombic and is in agreement with the findings of the previous workers.
- The excitation spectrum monitored at ~400 nm shows a broad band with one maximum at 280 nm.

- The feature of the excitation spectrum changed when monitored at ~ 470 nm shows a broad band with two maxima at 280 and 350 nm.
- These bands have been assigned as intra configurationally Ce^{4+}– O^{2-} charge transfer (CT) transitions.
- The emission spectra recorded on exciting at 254, 260, 280 as well as 350 nm show a broad band with the maximum in the blue–green region (FWHM~86) with extended emission into longer wavelengths.
- The emission spectrum of RE^{3+} ion doped Sr_2CeO_4 phosphor is composed of a broad band of lower intensity in the green-blue spectral region (which is already observed in the un-doped Sr_2CeO_4 phosphor) that overlaps with a set of Eu^{3+} intra-$^4f_6$ sharp lines in the blue, green and red regions.
- Fig.5 presents the scanning electron microscopy (SEM) images of un-doped and RE^{3+} (0.5mol %) ions doped Sr_2CeO_4 Phosphor. The entire sample exhibits grain like morphology with different sizes and shape.
- The present CIE Colour coordinates of (1931chart) the un-doped and RE^{3+} (0.5mol %) ions doped Sr_2CeO_4 Phosphor emitting with different colours like as blue, green, yellow and red regions under the excitation of 280, 350 nm respectively.
- These single host lattices emitting white light under UV and nUV excitations is an interesting phenomenon. Hence, these phosphors are multifunctional phosphors, which one can use according to the need.

5. Acknowledgment

One of the authors (Dr. Ch. Atchyutha Rao) is grateful for the financial support from the University Grant Commission (UGC), New Delhi, India, under Minor Research Project (MRP No: 4687/14-SERO/UGC), and the author expresses their sincere thanks to Prof. K. V. R. Murthy Garu to provide Lab facility in M.S. University, Baroda. Also very much thankful to the Principal GDC-Nakkapalli, ANAKAPALLE (Dt).

6. References

1. Yen WM, Weber MJ. Inorganic Phosphors - CRC Press. Boca Raton, FL (USA); c2004.
2. Blasse G, Grabmaier BC. Luminescent Materials, Springer-Verlag, Berlin, Germany; c1994.
3. Lakshmanan A. Nova Publishers, NY, USA, ISBN 978-1-60456-018-3; c2008.
4. Rao RP. Materials and Devices, Nova Science Publishers, Inc New York, NY (USA); c1992.
5. Van der Ziel JP, Van Uitert LG. J Appl. Phys.1986;60:4262.
6. Pollack SA, Chang DB, Moise NL. J Appl. Phys. 1986;60:4077.
7. France PW. (ed.) Optical Fiber Lasers and Amplifiers, CRC, Boca Raton, FL; c1991.
8. Zhang Chunxiang, Shi Jianshe, Yang Xujie, Wang Xin J of Rare earths. 2010;28:513-518.
9. Chang-Hsin Lu, Chang-Tao Chen. J sol-gel sci. Technol. 2007;43: -185.
10. Masui T, Chiga T, Imanaka N, Adachi G.-Y. Mater. Res. Bull. 2003;38:17- 24.
11. Jiao Hai- Yan, Wahg Yu-Hua, Zhang Jia-Chi J of Inorganic Materials. 2008;23**(**3):471-474.
12. Qiao Yanmin, Zhang Xinbo, *et al*. J of Rare earths. 2009;27(2):323-326.
13. Murthy K, Virk HS. In Luminescence phenomena- Trans Tech Pubs; c2014. p. 1-34.
14. Phosphor Handbook S. Shionoya and WM Yen. In CRC Press, Boca Raton; c1999.
15. Phosphor Hand book, second edition edited by William M. Yen, CRC press, Boca Raton; c2004.
16. Prabhu SS. E-Bayesian estimation of the shape parameter of Lomax model under symmetric and asymmetric loss functions. International Journal of Statistics and Applied Mathematics. 2020;5(6):142-146.
17. Color Calculator version 2, software from Radiant Imaging, Inc; c2007.
18. Sankar R, Subba Rao GV. Journal of electrochemical society. 2000;147:2773-2779.
19. Danielson E, Devenney M, Giaquinta DM. Science. 1998;279:837-839.
20. Serra OE, Severino VP. J. Alloys & Compounds. 2001, 323-324, 667-669.
21. Jiang YD, Zhang F. Appl. Phys. Letters. 1999;74(12):1677.
22. Danielson E, Devenney M, *et al*. Journal of Molecular Structure. 1998;470:229-235.
23. Chen SJ, Chen XT, Yu Z, Hong JM, Xue Z, You XZ. Solid State Commun. 2004;130:281-285.
24. Rao CA, Shakampally K, Murthy KVR. J Sci. Res. 2021;13(3):891-900.
25. Ch Atchyutha Rao N, Bujji Babu KVR. Murthy; J Adv Sci Res 2022;13(5):137-145.
26. Blasse G, Grabmaier BC. Luminescent Materials, Springer, Berlin, Germany; c1994.